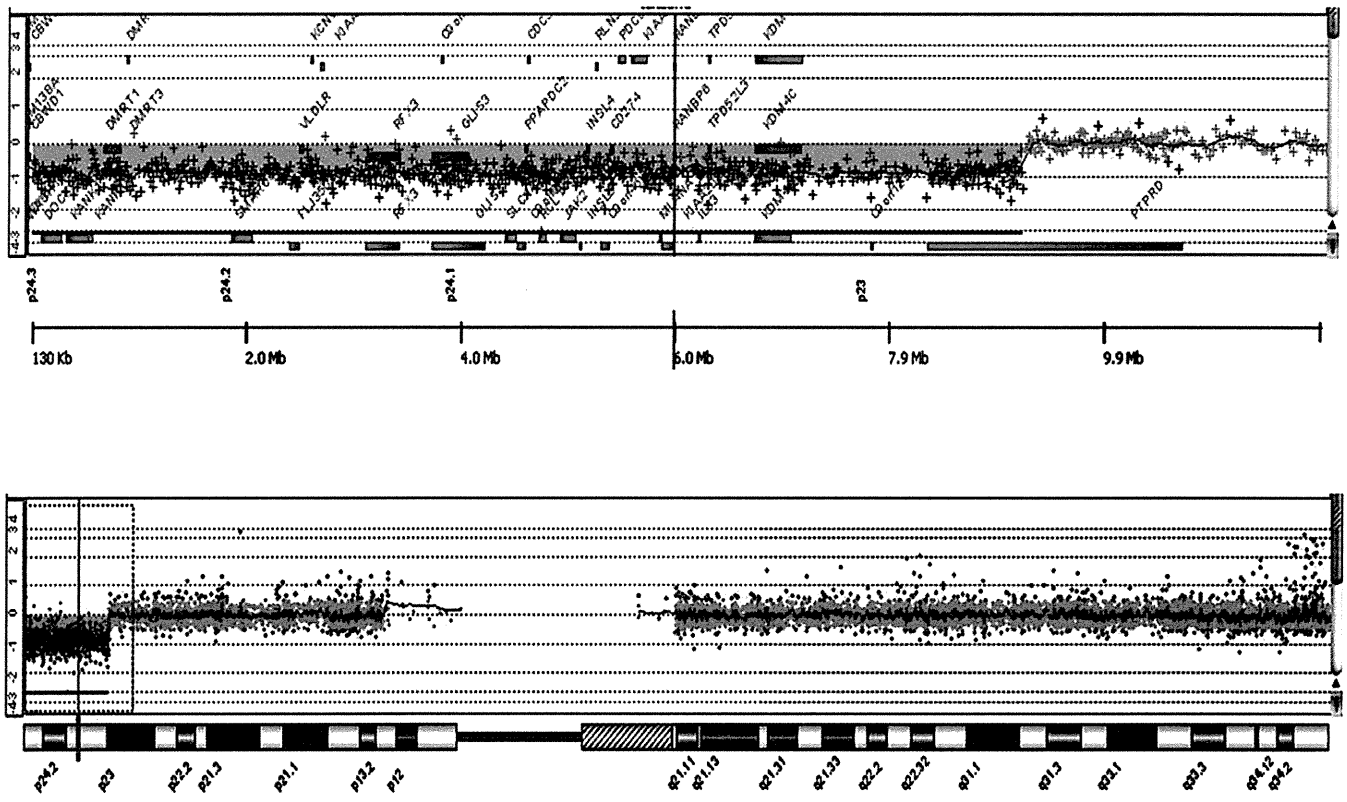

Fig. 3 Oligonucleotide array-CGH result of the patient. Whole chromosome view (lower) and close view (upper) of chromosome 9. Note a loss of 9.17 Mb of the terminal region of chromosome 9p.

Table 1 Fluoresence in situ hybridization (FISH) results using bacterial artificial chromosome clones and a subtelomeric probe around distal 9p

Probe name	Locus	Chromosome band	Distance from 9p terminal(Mb)	Signal on del(9p)
9p subtelomeric probe	–	9p24.3	–	–
RP11-143 M15	DMRT1	9p24.3	0.81	–
RP11-590E10	DMRT2	9p24.3	0.97	–
RP11-79 K3	–	9p24.1	7.30	–
RP11-29B9	D9S286	9p24.1	7.90	–
RP11-1134E16	D9S2000	9p23	8.99	–
RP11-74 L16	D9S912	9p23	9.26	+
RP11-176P17	D9S144	9p23	9.50	+
RP11-87N24	D9S168	9p23	10.47	+
RP11-58B8	–	9p23	11.60	+
RP11-382H24	D9S267	9p23	13.00	+

The distance from 9p terminal was retrieved from UCSC Genome Browser (NCBI 36/hg 18).

We compared deleted segments in all reported cases of 9p monosomy that were evaluated using molecular techniques (Fig. 4). Patients without trigonocephaly were not included in this comparison because penetrance of trigonocephaly might not be 100% and therefore considered unsuitable for use in phenotype mapping. While we could not find a common region that was shared by all patients, the segment from D9S912 to RP11-439I6, which is approximately 1 Mb, was deleted in the vast majority of the patients. There are only two patients who have a deletion that does not include this 1-Mb segment. The case reported by Kawara et al. (2006) had a more proximal interstitial deletion of 4.7 Mb at 9p22.3-p23. The chromosomal rearrangement in this patient was highly complex and

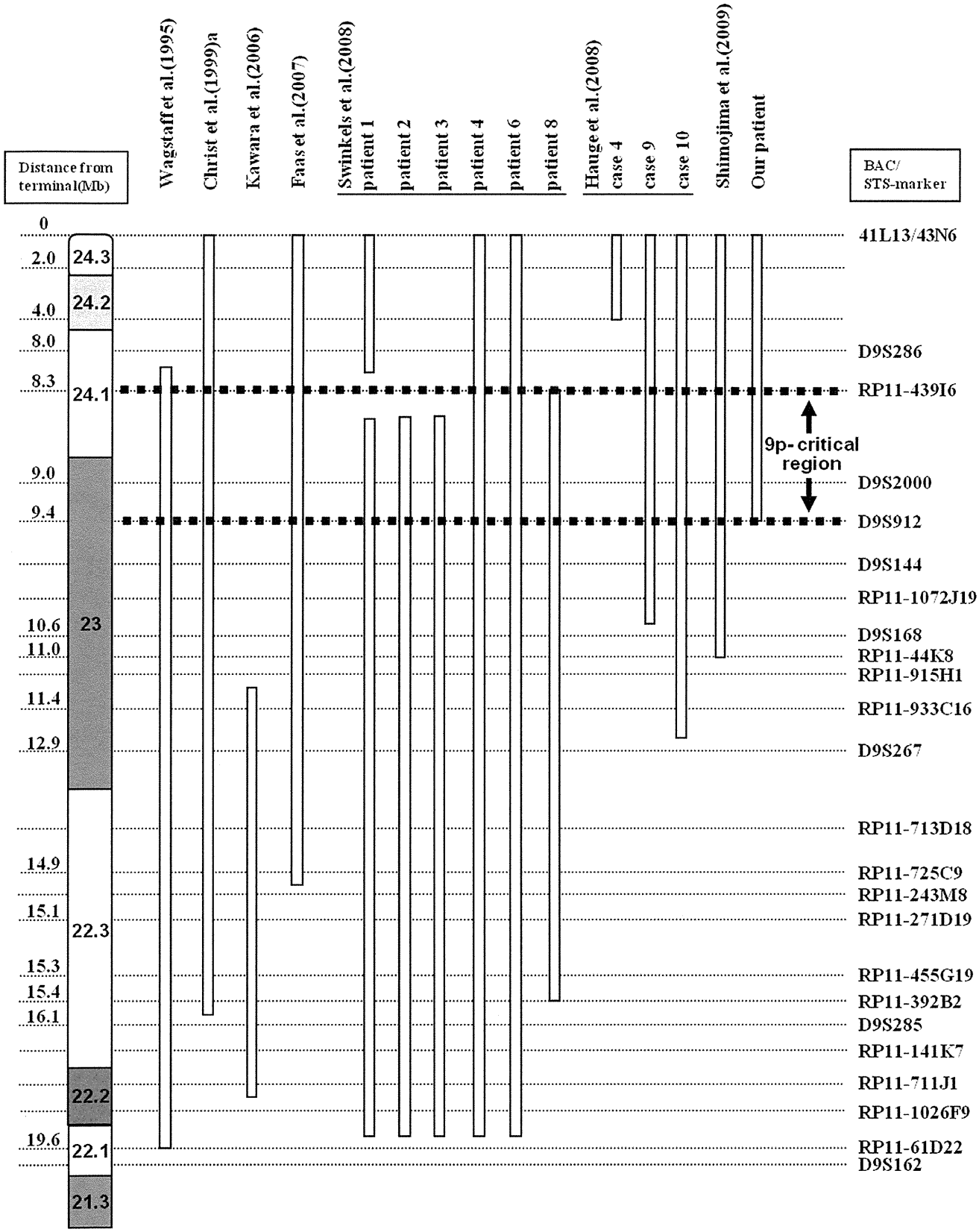

Fig. 4 Schematic map of the 9p deletion of reported cases of 9p monosomy, including the present case, evaluated using molecular analyses such as fluoresence in situ hybridization (FISH) and/or array comparative genomic hybridization. Open bars represent the presumed maximum extent of the deletion in each patient. a: the minimum common deleted region shared by 24 patients.

involved seven breakpoints on chromosomes 2 and 9. The patient, Case 4, reported by Hauge et al. (2008) showed a tiny terminal deletion of no more than 4 Mb. The karyotype of this patient was der(9)t(9;15) with a trisomic region from 15q(15q25-qter) that was translocated onto 9p24. That these two patients did not carry pure deletions of 9p may be noteworthy. Complex chromosome rearrangements are likely to have cryptic genome imbalance not only around the breakpoints but also at regions apart from the breakpoints. The altered chromosome constitution associated with unbalanced translocations might influence gene expression on the derivative chromosomes possibly through epigenetic modifications (Harewood et al. 2010). Obviously, it is preferable to choose pure terminal or interstitial deletion patients for genotype-phenotype mapping. In view of this preference and on the basis of comparison of deleted segments among patients with pure terminal or interstitial 9p deletion, including the present patient, we suggest the critical region for 9p monosomy syndrome, including trigonocephaly, might be a segment from D9S912 to RP11-439I6 of approximately 1 Mb. Of course, there are other possibilities: (i) the presence of multiple loci responsible for the syndrome and (ii) the presence of modifying factors that are located in different regions of the genome (Hauge et al. 2008). Further studies, such as using exome sequencing to screen cytogenetically normal patients with the 9p monosomy syndrome phenotype or with isolated trigonocephaly, might be necessary to identify the responsible gene for trigonocephaly of the 9p monosomy syndrome.

ACKNOWLEDGMENT

This study was funded in part by a grant from the Ministry of Health, Labour and Welfare, Japan, and from Kawano Masanori Memorial Foundation for Promotion of Pediatrics.

REFERENCES

Alfi O, Donnell GN, Crandall BF, Derencsenyi A, Menon R. 1973. Deletion of the short arm of chromosome no.9 (46,9p-): a new deletion syndrome. Ann Genet 16:17–22.

Barbaro M, Balsamo A, Anderlid BM et al. 2009. Characterization of deletions at 9p affecting the candidate regions for sex reversal and deletion 9p syndrome by MLPA. Eur J Hum Genet 17:1439–1447.

Christ LA, Crowe CA, Micale MA, Conroy JM, Schwartz S. 1999. Chromosome breakage hotspots and delineation of the critical region for the 9p-deletion syndrome. Am J Hum Genet 65:1387–1395.

Faas BH, de Leeuw N, Mieloo H, Bruinenberg J, de Vries BB. 2007. Further refinement of the candidate region for monosomy 9p syndrome. Am J Med Genet A 143A:2353–2356.

Harewood L, Schutz F, Boyle S et al. 2010. The effect of translocation-induced nuclear reorganization on gene expression. Genome Res 20:554–564.

Hauge X, Raca G, Cooper S et al. 2008. Detailed characterization of, and clinical correlations in, 10 patients with distal deletions of chromosome 9p. Genet Med 10:599–611.

Huret JL, Leonard C, Forestier B, Rethore MO, Lejeune J. 1988. Eleven new cases of del(9p) and features from 80 cases. J Med Genet 25:741–749.

Kawara H, Yamamoto T, Harada N et al. 2006. Narrowing candidate region for monosomy 9p syndrome to a 4.7-Mb segment at 9p22.2-p23. Am J Med Genet A 140:373–377.

Ogata T, Muroya K, Ohashi H, Mochizuki H, Hasegawa T, Kaji M. 2001. Female gonadal development in XX patients with distal 9p monosomy. Eur J Endocrinol 145:613–617.

Raymond CS, Shamu CE, Shen MM et al. 1998. Evidence for evolutionary conservation of sex-determining genes. Nature 391:691–695.

Shimojima K, Yamamoto T. 2009. Investigation of the candidate region for trigonocephaly in a patient with monosomy 9p syndrome using array-CGH. Am J Med Genet A 149A:1076–1080.

Swinkels ME, Simons A, Smeets DF et al. 2008. Clinical and cytogenetic characterization of 13 Dutch patients with deletion 9p syndrome: delineation of the critical region for a consensus phenotype. Am J Med Genet A 146A:1430–1438.

Wagstaff J, Hemann M. 1995. A familial 'balanced' 3;9 translocation with cryptic 8q insertion leading to deletion and duplication of 9p23 loci in siblings. Am J Hum Genet 56:302–309.

Focal Segmental Glomerulosclerosis in Patients With Complete Deletion of One *WT1* Allele

AUTHORS: Kazumoto Iijima, MD, PhD,[a] Tomonosuke Someya, MD, PhD,[b] Shuichi Ito, MD, PhD,[c] Kandai Nozu, MD, PhD,[a] Koichi Nakanishi, MD, PhD,[d] Kentaro Matsuoka, MD, PhD,[e] Hirofumi Ohashi, MD, PhD,[f] Michio Nagata; MD, PhD,[g] Koichi Kamei, MD, PhD,[c] and Satoshi Sasaki, MD, PhD[h]

[a]Department of Pediatrics, Kobe University Graduate School of Medicine, Kobe, Japan; [b]Department of Pediatrics, Juntendo University School of Medicine, Tokyo, Japan; [c]Departments of Nephrology and Rheumatology, and [e]Pathology, National Center for Child Health and Development, Tokyo, Japan; [d]Department of Pediatrics, Wakayama Medical University, Wakayama, Japan; [f]Division of Medical Genetics, Saitama Children's Medical Center, Saitama, Japan; [g]Department of Pathology, Institute of Basic Medical Sciences, University of Tsukuba, Tsukuba, Japan; and [h]Department of Pediatrics, Hokkaido University Graduate School of Medicine, Sapporo, Japan

KEY WORDS
deletion, focal segmental glomerulosclerosis, WAGR syndrome, *WT1*

ABBREVIATIONS
ACEI—angiotensin-converting enzyme inhibitor
BUN—blood urea nitrogen
CrCl—creatinine clearance
DDS—Denys-Drash syndrome
DMS—diffuse mesangial sclerosis
FSGS—focal segmental glomerulosclerosis
WAGR—Wilms' tumor, aniridia, genitourinary anomalies, and mental retardation

Each author contributed to the study as follows: Dr Iijima, patient management and manuscript writing; Dr Someya, patient management; Dr Ito, patient management; Dr Nozu, genetic analysis; Dr Nakanishi, genetic analysis; Dr Matsuoka, pathological analysis; Dr Ohashi, genetic analysis; Dr Nagata, pathological analysis; Dr Kamei, patient management; and Dr Sasaki, patient management.

www.pediatrics.org/cgi/doi/10.1542/peds.2011-1323

doi:10.1542/peds.2011-1323

Accepted for publication Jan 11, 2012

Address correspondence to Kazumoto Iijima, MD, PhD, Department of Pediatrics, Kobe University Graduate School of Medicine, 7-5-2 Kusunoki-Cho, Chuo-ku, Kobe 650–0017, Japan. E-mail: iijima@med.kobe-u.ac.jp

PEDIATRICS (ISSN Numbers: Print, 0031-4005; Online, 1098-4275).

FINANCIAL DISCLOSURE: *The authors have indicated they have no financial relationships relevant to this article to disclose.*

FUNDING: This study was supported by Grants-in-Aid for Scientific Research (B) (to Dr Iijima, 20390240) from the Japan Society for the Promotion of Science.

abstract

The renal prognosis of patients with Wilms' tumor, aniridia, genitourinary anomalies, and mental retardation syndrome (WAGR) is poor. However, the renal histology and its mechanisms are not well understood. We performed renal biopsies in 3 patients with WAGR syndrome who had heavy proteinuria. The complete deletion of one *WT1* allele was detected in each patient by constitutional chromosomal deletion at 11p13 using G-banding, high-resolution G-banding, and fluorescence in situ hybridization. The patients exhibited proteinuria at the ages of 6, 10, and 6 years and were diagnosed as having focal segmental glomerulosclerosis (FSGS) at the ages of 7, 16 and 19 years, respectively. They exhibited normal or mildly declined renal function at the time of biopsy. Re-examination of a nephrectomized kidney from 1 patient revealed that some glomeruli showed segmental sclerosis, although he did not have proteinuria at the time of nephrectomy. The other 2 patients did not develop Wilms' tumor and thus did not undergo nephrectomy, chemotherapy, or radiotherapy, thereby eliminating any effect of these therapies on the renal histology. In conclusion, complete deletion of one *WT1* allele may induce the development of FSGS. Our findings suggest that haploinsufficiency of the *WT1* could be responsible for the development of FSGS. *Pediatrics* 2012;129:e1621–e1625

Miller et al[1] first described WAGR syndrome (Wilms' tumor, aniridia, genitourinary anomalies, and mental retardation). Children with WAGR syndrome invariably have a constitutional chromosomal deletion at 11p13, the region where the *WT1* gene is located. Patients with Denys-Drash syndrome (DDS) usually have a germline missense mutation, which is predicted to result in an amino acid substitution in the eighth or ninth exon of *WT1*. Little et al[2] suggested that the severe nephropathy associated with DDS, which frequently leads to early renal failure, might result from the dominant-negative action of altered *WT1*. By contrast, because of the less severe genital anomalies and apparent lack of nephropathy associated with WAGR, a reduced *WT1* dosage during embryogenesis is thought to have a less pronounced effect on development, especially on renal system development.[3] Breslow et al[4] reviewed nearly 6000 patients enrolled in 4 clinical trials administered by the US National Wilms Tumor Study Group between 1969 and 1995. Of 22 patients with DDS, 13 (59%) developed renal failure; of 46 patients with WAGR, 10 (22%) developed renal failure. The cumulative risks of renal failure at 20 years were 62% and 38%, respectively. These findings suggest that nephropathy is not uniquely associated with missense mutations in *WT1* and that patients with the WAGR syndrome should be followed up closely throughout life for signs of nephropathy.

The renal prognosis of patients with WAGR is poor. However, the renal histology and its mechanisms are not well understood. We therefore performed renal biopsies to reveal the renal pathology in 3 patients with WAGR syndrome who had heavy proteinuria.

CASE REPORTS

Patient 1

Patient 1 was a male diagnosed with bilateral microphthalmos at 1 month of age. Wilms' tumor developed bilaterally at 3 years of age. He also had undescended testes and mental retardation. Previous analysis of G-banded metaphase chromosomes revealed a deletion of chromosome 11p13-15.1 in one allele[5]; the diagnosis of atypical WAGR syndrome was therefore made.[6] Because of a large tumor in the right kidney after the first chemotherapy treatment, the right kidney was nephrectomized. A diagnosis of nephroblastoma (nephroblastic type) was made. At the same time, the contralateral left kidney was biopsied, but no tumor was detected. The nephrectomized kidney revealed that there were no immature glomeruli, and a few glomeruli showed segmental sclerosis (Fig 1 A and B). The patient did not have proteinuria at the time of nephrectomy although microalbuminuria could have been detected.

The patient then underwent a second session of chemotherapy and radiotherapy treatment with left kidney protection. He developed heavy proteinuria at 6 years of age. The left kidney was biopsied (open biopsy) at age 7 years. Renal biopsy findings were consistent with focal segmental glomerulosclerosis (FSGS) (Fig 1 C and D). At the time of biopsy, the patient's height was 107.3 cm (–2.9 SD), weight was 21.7 kg (–0.7 SD), and blood pressure was 120/80 mm Hg. Biochemical data were as follows: total protein, 6.5 g/dL; albumin, 3.3 g/dL; blood urea nitrogen (BUN), 12.9 mg/dL; creatinine, 0.43 mg/dL; 24-hour creatinine clearance (CrCl), 72.2 mL/min/1.73 m^2; early morning urinary protein, 3+ (as measured by using a dipstick test); urinary protein to urinary creatinine ratio, 3.6 (milligram/milligram); and urinary β-2 microglobulin, 0.44 mg/dL (normal range: <0.23 mg/dL). His renal function gradually deteriorated despite angiotensin-converting enzyme inhibitor (ACEI) treatment. At 14 years of age, he underwent a preemptive living-related renal transplantation from his father.

Patient 2

Patient 2 was a male with aniridia, bilateral undescended testes, hypospadias, grade III to IV bilateral vesicoureteral reflux, and mental retardation. High-resolution G-banding revealed deletion of chromosome 11p13-p14.2 in one allele (Fig 2A), and fluorescence in situ hybridization showed heterozygous deletions of *PAX6*, *D11S2163*, *PER*, and *WT1* (Fig 2B), indicating WAGR syndrome. He had a single febrile urinary tract infection at 2 years of age and underwent an antireflux operation at 4 years of age, which resolved his vesicoureteral reflux. A dimercaptosuccinic acid radionuclide scan showed several defects in his right kidney. His proteinuria was detected at 10 years of age by the school urinary screening program. His proteinuria gradually increased, and he underwent renal biopsy (right kidney) at age 16 years. Renal biopsy findings were consistent with FSGS (Fig 1 E and F). At the time of biopsy, the patient's height was 169.2 cm, weight was 67.4 kg, and blood pressure was 128/78 mm Hg. Biochemical data were as follows: total protein, 6.8 g/dL; albumin, 4.3 g/dL; BUN, 25.0 mg/dL; creatinine, 1.20 mg/dL; 24-hour CrCl, 91.0 mL/min/1.73 m^2; early morning urinary protein, 3+ (as measured by using a dipstick test); urinary protein to urinary creatinine ratio, 2.7 (milligram/milligram); daily urinary protein, 3.1 g; and urinary β-2 microglobulin, 0.064 mg/dL. At the latest follow-up (24 years of age), his renal function was stable (BUN: 25.0 mg/dL; creatinine: 1.20 mg/dL) with ACEI treatment, and he had not developed Wilms' tumor.

Patient 3

Patient 3 was a female with aniridia and mental retardation. G-banding revealed deletion of chromosome 11p13-p14 in one allele (Fig 2C), and she was therefore diagnosed with WAGR syndrome. The patient developed proteinuria at

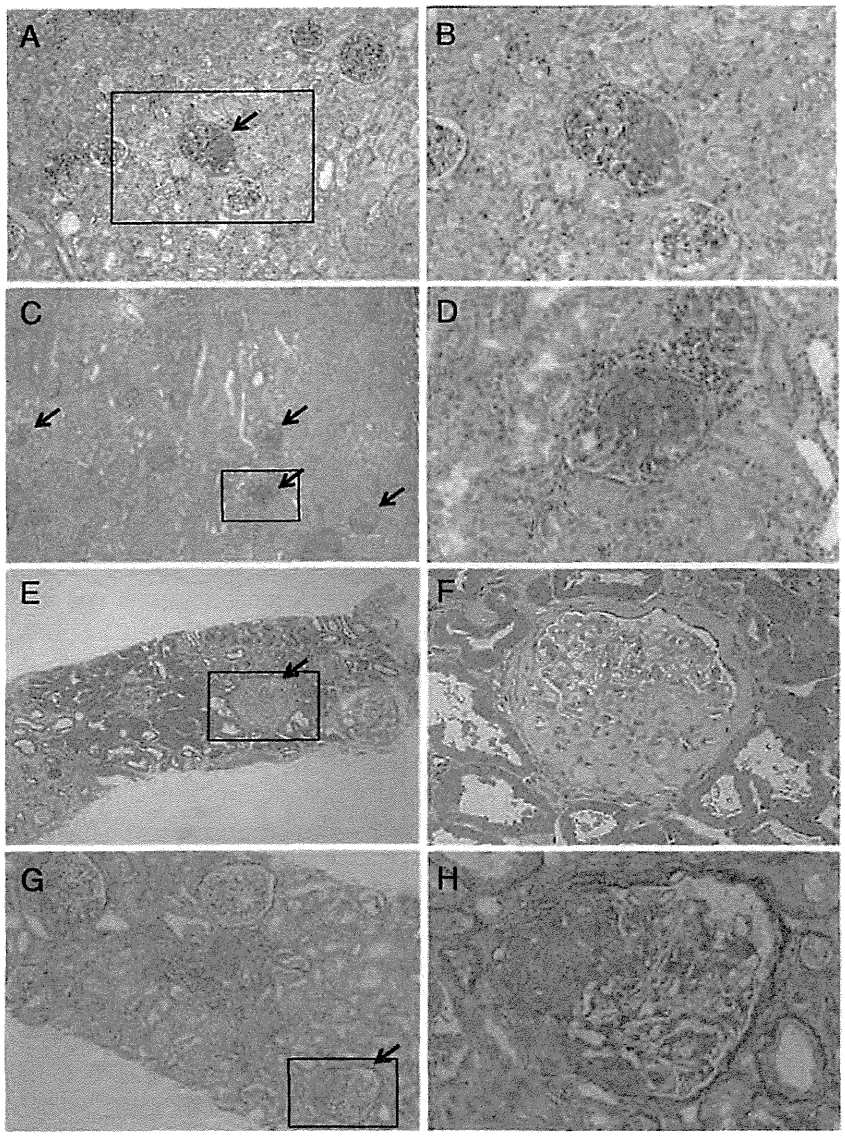

FIGURE 1

Renal histology. A, C, E, and G, Low magnification. B, D, F, and H, High magnification. Arrows show glomeruli with segmental glomerulosclerosis. A and B, Nephrectomized right kidney from patient 1. Patient 1 had no proteinuria at the time of nephrectomy. However, a few glomeruli exhibited segmental glomerulosclerosis although there were no immature glomeruli. C and D, Renal biopsy of left kidney from patient 1. Twenty-eight of 50 glomeruli showed segmental glomerulosclerosis. There were no tubulointerstitial lesions. E and F, Renal biopsy from patient 2. Two of eight glomeruli showed segmental glomerulosclerosis with interstitial fibrosis. G and H, Renal biopsy from patient 3. Ten of 30 glomeruli showed segmental glomerulosclerosis with interstitial fibrosis. All 3 patients exhibited FSGS (not otherwise specified).

the age of 6 years and nephrotic syndrome with normal renal function at age 15 years (urinary protein to urinary creatinine ratio, 10.6 [milligram/milligram]; total protein, 5.6 g/dL; albumin, 2.3 g/dL; BUN, 15.0 mg/dL; creatinine, 0.65 mg/dL; estimated glomerular filtration rate, 100.7 mL/min/1.73 m^2). We were unable to obtain her parents' consent for renal biopsy, and they chose to start drug treatment. However, treatment with prednisolone and ACEI was not effective, and her renal function gradually deteriorated. Therefore, she underwent renal biopsy at age 19 years. At the time of biopsy, her height was 144.5 cm, weight was 72.5 kg, and blood pressure was 130/83 mm Hg. Biochemical data were as follows: total protein, 5.5 g/dL; albumin, 2.5 g/dL; BUN, 30.0 mg/dL; creatinine, 1.40 mg/dL; 24-hour CrCl, 44.65 mL/min/1.73 m^2; early morning urinary protein, 3+ (as measured by using a dipstick test); daily urinary protein, 5.89 g; and urinary β-2 microglobulin, 0.495 mg/dL. Renal biopsy findings were consistent with FSGS (Fig 1 G and H). To date, she has not developed Wilms' tumor.

DISCUSSION

The current study demonstrated that 3 patients with atypical WAGR syndrome developed heavy proteinuria with FSGS, suggesting that the nephropathy seen in this syndrome is responsible for the FSGS lesion.

Patient 1 had possible bilateral Wilms' tumor and underwent unilateral nephrectomy, chemotherapy, and radiotherapy. Therefore, it is possible that the treatment of the remaining kidney for bilateral tumor or nephrogenic rest might account for the development of FSGS. However, the kidney nephrectomized after the first chemotherapy session but before radiotherapy treatment already showed segmental sclerosis in a few glomeruli, suggesting that radiotherapy was not the main cause of FSGS. Chemotherapeutic drugs such as adriamycin may induce FSGS as well as tubulointerstitial inflammation and fibrosis.[7] However, there were no tubulointerstitial lesions, suggesting that chemotherapy might not have been the main cause of FSGS. Nevertheless, it is possible that surgical renal ablation caused FSGS in patient 1.

Patients 2 and 3 did not develop Wilms' tumor during the course of clinical observation, and thus they did not undergo nephrectomy, chemotherapy, or radiotherapy, thereby eliminating any effect of these therapies on renal

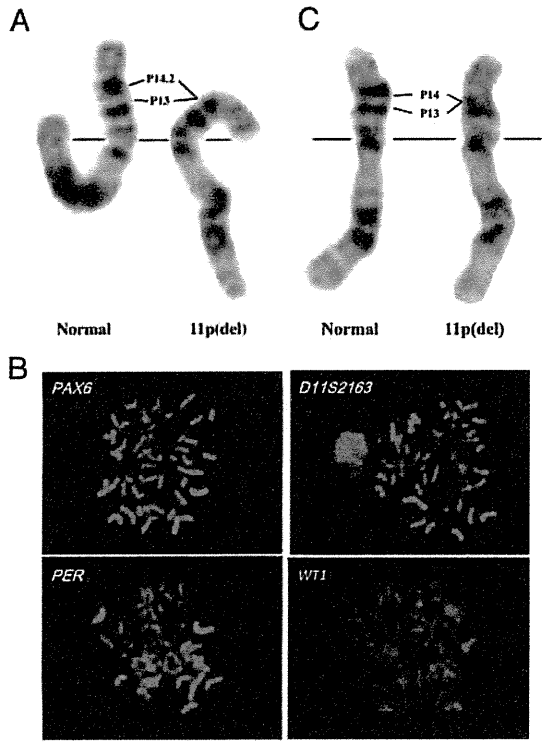

FIGURE 2

High-resolution G-banding of chromosome 11 and fluorescence in situ hybridization (FISH) in patient 2 and G-banding of chromosome 11 in patient 3. A, Patient 2 had deletion of chromosome 11p13-p14.2 in one allele. B, FISH using P1-derived artificial chromosome clones (1083G3 for *PAX6*; 65P5 for *D11S2163*; 685F3 for *PER*; and 104M13 for *WT1*) as probes was performed for patient 2, as previously reported.[6] Each FISH signal for *PAX6, D11S2163, PER, and WT1* was observed in only one chromosome 11 homolog, indicating heterozygous deletion of the WAGR region of 11p. C, Patient 3 had deletion of chromosome 11p13-p14 in one allele.

histology. The possibility of reflux nephropathy, however, could not be ruled out in patient 2. The perihilar variant with glomerular hypertrophy is particularly common in the secondary FSGS such as reduced renal mass–induced FSGS.[8] However, all 3 patients exhibited FSGS (not otherwise specified) without glomerular hypertrophy, suggesting that surgical renal ablation (patient 1) and reflux nephropathy (patient 2) may not have been the main cause of FSGS in these 2 patients. These findings suggest that the complete deletion of one *WT1* allele might have a pathogenetic role in the development of nephropathy.

The spectrum of glomerular diseases associated with *WT1* mutations has been reviewed.[9] *WT1* mutations can cause syndromic and nonsyndromic glomerular disease. The syndromic forms include DDS (early-onset nephrotic syndrome with diffuse mesangial sclerosis [DMS]); 46,XY disorders of sex development and Wilms' tumor; and Frasier syndrome (disorders of sex development, FSGS, and gonadoblastoma), which is caused by a mutation in the intron 9 splice site of *WT1* leading to the loss of the +KTS isoform of the protein. Mutations associated with both syndromic and nonsyndromic glomerular disease tend to cluster in exons 8 and 9 of *WT1*, which encode zinc fingers 2 and 3.[9,10] Orloff et al[11] reported that single-nucleotide polymorphisms in *WT1* may modulate the development of FSGS by altering *WT1* function. The current study suggests that complete deletion of one *WT1* allele may also induce the development of nephropathy.

Reduced expression levels of *Wt1*-induced glomerulopathies (crescentic glomerulonephritis or DMS) depending on gene dosage derived by combining *Wt1*-knockout mice and an inducible *Wt1* yeast artificial chromosome transgenic mouse model.[12] Eleven percent of mice heterozygous for the *Wt1* mutation showed severe proteinuria and DMS with tubular cysts, protein casts, and severe interstitial inflammation, although nephrogenesis was not delayed.[12] These findings indicate that the expression level of *WT1* plays an important role, not only during nephrogenesis but also in the homeostasis of normal kidney function. These findings also support our conclusion that complete deletion of one *WT1* allele in atypical WAGR syndrome could induce glomerulopathy without delayed nephrogenesis, although the reason for the discrepancy in histologic findings between man (FSGS) and mouse (DMS) is unclear.

CONCLUSIONS

Besides dominant-negative missense mutations in the eighth or ninth exon of *WT1* and mutations at the donor splice site of intron 9, complete deletion of one *WT1* allele may induce the development of FSGS. The findings in this study also suggest that haploinsufficiency of *WT1* could be responsible for the development of FSGS.

REFERENCES

1. Miller RW, Fraumeni JF Jr, Manning MD. Association of Wilms' tumor with aniridia, hemihypertrophy and other congenital malformations. *N Engl J Med.* 1964;270:922–927
2. Little MH, Williamson KA, Mannens M, et al. Evidence that WT1 mutations in Denys-

Drash syndrome patients may act in a dominant-negative fashion. *Hum Mol Genet.* 1993;2(3):259–264

3. Huff V. Genotype/phenotype correlations in Wilms' tumor. *Med Pediatr Oncol.* 1996;27 (5):408–414
4. Breslow NE, Takashima JR, Ritchey ML, Strong LC, Green DM. Renal failure in the Denys-Drash and Wilms' tumor-aniridia syndromes. *Cancer Res.* 2000;60(15):4030–4032
5. Kawase E, Tanaka K, Honna T, Azuma N. A case of atypical WAGR syndrome with anterior segment anomaly and microphthalmos. *Arch Ophthalmol.* 2001;119(12): 1855–1856
6. Muto R, Yamamori S, Ohashi H, Osawa M. Prediction by FISH analysis of the occurrence of Wilms tumor in aniridia patients. *Am J Med Genet.* 2002;108(4):285–289
7. Lee VW, Harris DC. Adriamycin nephropathy: a model of focal segmental glomerulosclerosis. *Nephrology (Carlton).* 2011;16 (1):30–38
8. D'Agati VD. The spectrum of focal segmental glomerulosclerosis: new insights. *Curr Opin Nephrol Hypertens.* 2008;17(3):271–281
9. Niaudet P, Gubler MC. WT1 and glomerular diseases. *Pediatr Nephrol.* 2006;21(11): 1653–1660
10. Mucha B, Ozaltin F, Hinkes BG, et al; Members of the APN Study Group. Mutations in the Wilms' tumor 1 gene cause isolated steroid resistant nephrotic syndrome and occur in exons 8 and 9. *Pediatr Res.* 2006; 59(2):325–331
11. Orloff MS, Iyengar SK, Winkler CA, et al. Variants in the Wilms' tumor gene are associated with focal segmental glomerulosclerosis in the African American population. *Physiol Genomics.* 2005;21(2): 212–221
12. Guo JK, Menke AL, Gubler MC, et al. WT1 is a key regulator of podocyte function: reduced expression levels cause crescentic glomerulonephritis and mesangial sclerosis. *Hum Mol Genet.* 2002;11(6): 651–659

Journal of Human Genetics (2012) 00, 1–8

www.nature.com/jhg

ORIGINAL ARTICLE

Subtelomeric deletions of 1q43q44 and severe brain impairment associated with delayed myelination

Keiko Shimojima[1], Nobuhiko Okamoto[2], Yume Suzuki[3], Mari Saito[3], Masato Mori[3], Tatanori Yamagata[3], Mariko Y Momoi[3], Hideji Hattori[4], Yoshiyuki Okano[4], Ken Hisata[5], Akihisa Okumura[5] and Toshiyuki Yamamoto[1]

Subtelomeric deletions of 1q44 cause mental retardation, developmental delay and brain anomalies, including abnormalities of the corpus callosum (ACC) and microcephaly in most patients. We report the cases of six patients with 1q44 deletions; two patients with interstitial deletions of 1q44; and four patients with terminal deletions of 1q. One of the patients showed an unbalanced translocation between chromosome 5. All the deletion regions overlapped with previously reported critical regions for ACC, microcephaly and seizures, indicating the recurrent nature of the core phenotypic features of 1q44 deletions. The four patients with terminal deletions of 1q exhibited severe volume loss in the brain as compared with patients who harbored interstitial deletions of 1q44. This indicated that telomeric regions have a role in severe volume loss of the brain. In addition, two patients with terminal deletions of 1q43, beyond the critical region for 1q44 deletion syndrome exhibited delayed myelination. As the deletion regions identified in these patients extended toward centromere, we conclude that the genes responsible for delayed myelination may be located in the neighboring region of 1q43.
Journal of Human Genetics advance online publication, 21 June 2012; doi:10.1038/jhg.2012.77

Keywords: 1q44 deletion; abnormalities of the corpus callosum; *AKT3*; delayed myelination; microcephaly; subtelomeric deletion; *ZNF238*

INTRODUCTION

Submicroscopic subtelomeric chromosomal deletions have been found in 7.4% of children with moderate to severe mental retardation.[1] Some subtelomeric deletion syndromes are clinically recognizable and identified by characteristic features, whereas some others cannot be identified by such means. The recent development of molecular karyotyping using chromosomal microarray testing has revealed clear genotype–phenotype correlations and identified the critical chromosomal regions of the characteristic features of subtelomeric deletions. The most striking example is the Miller-Diecker syndrome, which has shown clear genotype–phenotype correlations.[2] Miller-Diecker syndrome is caused by the subtelomeric deletion of 17p, and is well recognized and characterized by lissencephaly and distinctive facial features,[3] which result from the involvement of the platelet-activating factor acetylhydrolase 1b regulatory subunit 1 gene (*PAFAH1B1*) and tyrosine 3-monooxygenase/tryptophan 5-monooxygenase-activation protein epsilon polypeptide gene (*YWHAE*), respectively; both these genes are located on 17p13.[3]

Several studies have investigated the critical region for 1q44 subtelomeric deletion syndrome and found that the core phenotypic features of 1q44 subtelomeric deletion syndrome are microcephaly, abnormalities of the corpus callosum (ACC) and seizures.[4–16] Recently, Ballif *et al.*[17] analyzed patients with microdeletions of 1q44 and proposed certain genes that may be responsible for individual features.

We report the cases of six newly identified patients with 1q44 deletions; two with interstitial deletion of 1q44; and four with terminal deletion of 1q. As the patients with terminal deletion of 1q44 exhibited more severe phenotypes compared with the patients with interstitial deletion, the phenotypic differences would be derived from additionally deleted region of 1q43q44.

MATERIALS AND METHODS

Subjects

Six Japanese patients were diagnosed as having chromosomal deletions in the region of 1q43q44 in our ongoing study to analyze genomic copy number aberrations. This study was approved by the ethical committee of our institution. After obtaining written consents, we accumulated samples from the patients. Parental samples were also obtained to study their carrier status.

[1]Tokyo Women's Medical University Institute for Integrated Medical Sciences (TIIMS), Tokyo, Japan; [2]Department of Medical Genetics, Osaka Medical Center and Research Institute for Maternal and Child Health, Izumi, Japan; [3]Department of Pediatrics, Jichi Medical University, Shimotsuke, Japan; [4]Department of Pediatrics, Osaka City University School of Medicine, Osaka, Japan and [5]Department of Pediatrics, Juntendo University School of Medicine, Tokyo, Japan
Correspondence: Dr T Yamamoto, Tokyo Women's Medical University Institute for Integrated Medical Sciences (TIIMS), 8-1 Kawada-cho, Shinjuku-ward, Tokyo 162-8666, Japan.
E-mail: yamamoto.toshiyuki@twmu.ac.jp
Received 10 April 2012; revised 24 May 2012; accepted 25 May 2012

Methods

Genomic copy number was analyzed using the 244, 105 or 60 K Human Genome CGH Microarray (Agilent Technologies, Santa Clara, CA, USA) as described previously.[2] Genomic DNAs was extracted from peripheral blood using a standard method. Genomic copy number aberrations were visualized using Agilent Genomic Workbench version 5.5 (Agilent Technologies).

Fluorescence *in situ* hybridization (FISH) was performed as previously described, when metaphase spreads were available.[2] Bacterial artificial clones were selected from the UCSC genome browser (http://www.genome.ucsc.edu). Physical positions refer to the March 2009 human reference sequence. Bacterial artificial clone DNAs were extracted by an automatic DNA extraction system GENE PREP STAR PI-80X (Kurabo, Osaka, Japan).

RESULTS

Chromosomal deletions

Chromosomal microarray testing revealed aberrations in the 1q43q44 region in six patients (Figure 1). In patient 1 and 2, interstitial deletions of 1.9 and 2.2 Mb, respectively, were identified within the 1q43q44 region. In patient 1, FISH analysis confirmed the deletion (Figure 2a). Subsequent FISH analysis revealed no abnormalities in the parents of both families, indicating *de novo* deletions in both patients. Molecular karyotyping defined the aberrations as arr 1q44(243 809 193–245 665 521) × 1 dn for patient 1 and arr 1q43q44(243 303 991–245 506 920) × 1 dn for patient 2.

In patient 3, terminal deletions of 1q43 were identified and confirmed by FISH analyses (Figure 2b). As FISH analyses for both parents showed no abnormalities, this deletion occurred as *de novo*. Molecular karyotyping of patient 3 was indicated as arr 1q43q44(242 442 098–249 250 621) × 1 dn.

In patient 4, a loss of genomic copy number at 1q43q44 and an additional gain at 5p15.33 were identified (Supplementary Figure 1). Subsequent FISH analysis confirmed an unbalanced translocation between 1q43 and 5p in patient 4 (Figures 2c–e), and no translocation was found in either parents. Consequently, the patient's unbalance translocation was determined to be *de novo* in origin. Her karyotype was 46,XX,der(1)t(1;5)(q43;p15.33).arr 1q43q44(242 223 230–249 212 668) × 1, 5p15.33(57 640–1 705 515) × 3 dn. The duplicated region of 5p was only 1.7 Mb of the terminal region.

In patient 5, terminal deletions of 1q43 were identified with a breakpoint in the v-akt murine thymoma viral oncogene homolog 3 gene (*AKT3*). The molecular karyotype was arr 1q44(243 880 099–249 212 668) × 1. The largest deletion was identified in patient 6 with arr 1q43q44(238 888 870–249 212 668) × 1.

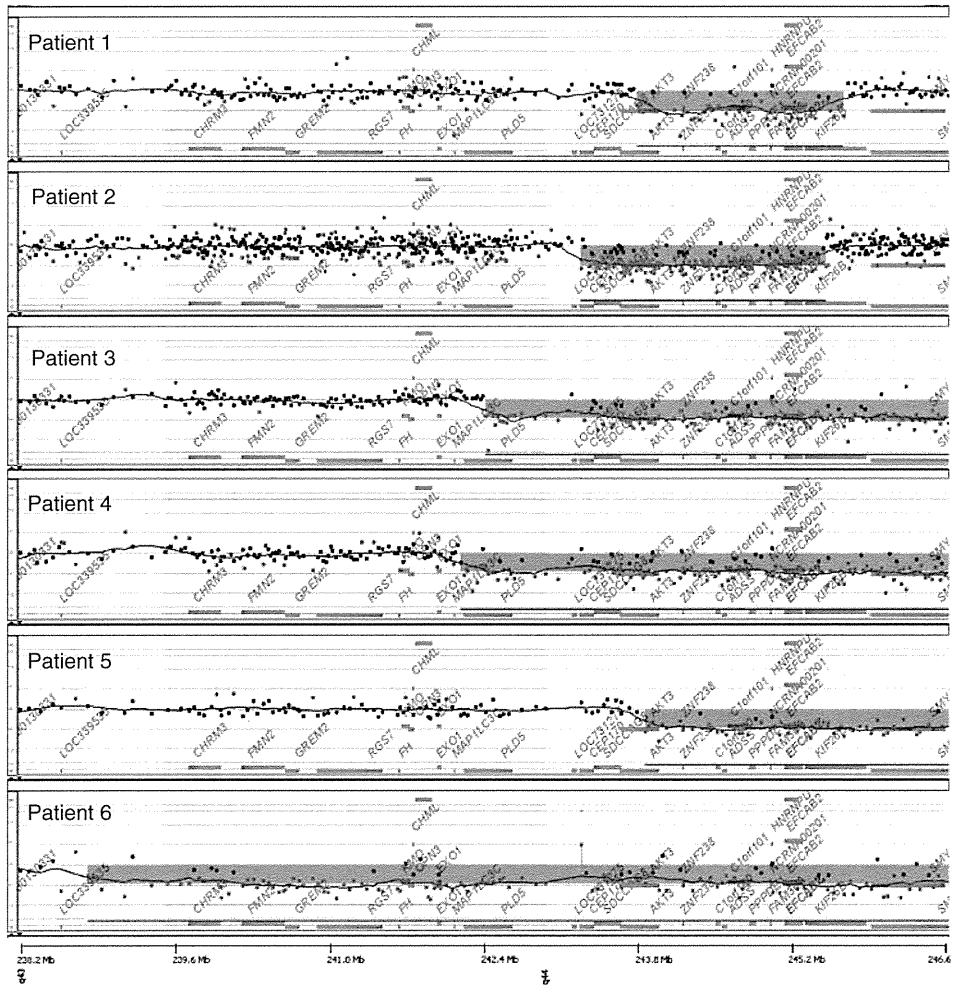

Figure 1 Results of chromosomal microarray testing presented by Gene View of Agilent Genomic Workbench (Agilent Technologies). Vertical axis and horizontal axis represent $\log_2$ signal ratio and genomic position, respectively. Aberrant regions are shown by blue rectangles. Dots indicate the genomic positions and the $\log_2$ ratio of each probe.

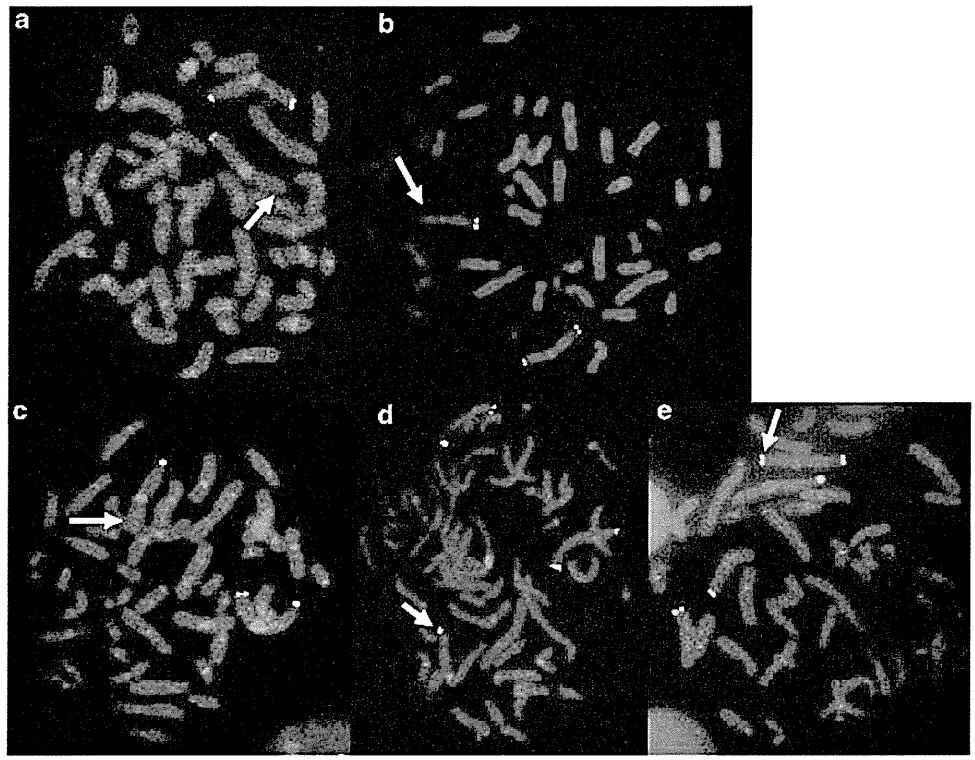

Figure 2 Results of FISH analyses. (**a**) Loss of the green signal labeling RP11-7L23 (arrow) indicates deletion of 1q44 in patient 1. (**b**) Loss of the green signal labeling RP11-88N11 (arrow) indicates deletion of 1q44 in patient 3. (**c–e**) Confirmation of the unbalanced translocation between chromosome 1 and 5 in patient 4. Loss of the green signal labeling RP11-143E8 (arrow) indicates deletion of 1q44 (**c**). An additional signal labeling RP11-94J21 of 5p15.33 is present on the other chromosome (**d**, red signal, arrow), indicating a translocation onto chromosome 1 (**e**, green signal, arrow).

The result of FISH analysis were summarized in Supplementary Table 1.

CLINICAL REPORT

Patient 1

A 9-year-old boy was born by vacuum extraction. His birth weight was 2820 g (within 25th centile), length was 45 cm (= 3rd centile) and occipitofrontal circumference (OFC) was 32.5 cm (10–25th centile). After birth, he displayed feeding problem. His development was mildly delayed with head control attained at 8 months, sitting without support at 15 months, crawling at 24 months and walking alone without support at 44 months. At the age of 11 months, he experienced recurrent febrile seizures. At 18 months of age, he suffered non-febrile seizures. The brain magnetic resonance imaging (MRI) at 4 years of age revealed loss of volume in the frontal lobe, mild abnormal gyral patterns in the frontal lobe and lateral lobe, and ACC (Figures 3a–c). Conventional chromosomal analysis revealed a normal male karyotype.

At present, his height is 119.5 cm (<3rd centile) and weight is 23.6 kg (10th centile). He exhibits microcephaly with OFC of 47.5 cm (<3rd centile). He displays distinctive facial features including a flat occipit, coarse face, high nasal bridge, low-set ears and prominent jaw (Figure 4a). He has short tapering fingers and single palmer creases.

Patient 2

A 3-year and 1-month-old girl is a second child of healthy non-consanguineous parents with an unremarkable family history. She was born at 36th week of gestation after an uneventful pregnancy. She displayed prenatal growth retardation with her weight of 2348 g (<3rd centile), length of 44.4 cm (<3rd centile) and OFC of 31 cm (<3rd centile). At the age of 6 months, developmental delay and microcephaly were noted. She could balance her head at 6 months, sit at 10 months, roll over at 13 months and crawl at 20 months. At the age of 11 months, she suffered febrile convulsion, followed by 11 recurrent attacks of complex febrile seizures. The findings of her electroencephalogram were unremarkable.

At the age of 2 years and 11 months, she had a short stature (height 79 cm, <3rd centile; weight 10 kg, <3rd centile) and microcephaly (OFC 42.5 cm, <3rd centile). Facial dysmorphism included epicanthal folds, a broad nasal root and down-turned corner of mouth (Figure 4b). Neurological examination revealed generalized hypotonia. At this time, she showed moderate psychomotor developmental delay with motor development of 10 months and language development of 8 months. Ultrasonography of the kidneys and liver, echocardiography, ophthalmologic and audiologic examinations revealed no abnormalities. Conventional chromosome analysis revealed a normal female karyotype.

At present, the patient cannot stand without support. She can speak only babbled words. The brain MRI revealed ACC and loss of the volume of the frontal lobe (Figures 3d–f).

Patient 3

A 1-year and 6-month-old girl was born at the gestational age of 38 weeks by vaginal delivery. Although her pregnancy was unremarkable, she showed prenatal growth retardation with her birth weight of 2040 g (<3rd centile) and OFC of 30 cm (<3rd centile). Her APGAR score was 9/9. One hour after birth, she suffered a convulsion

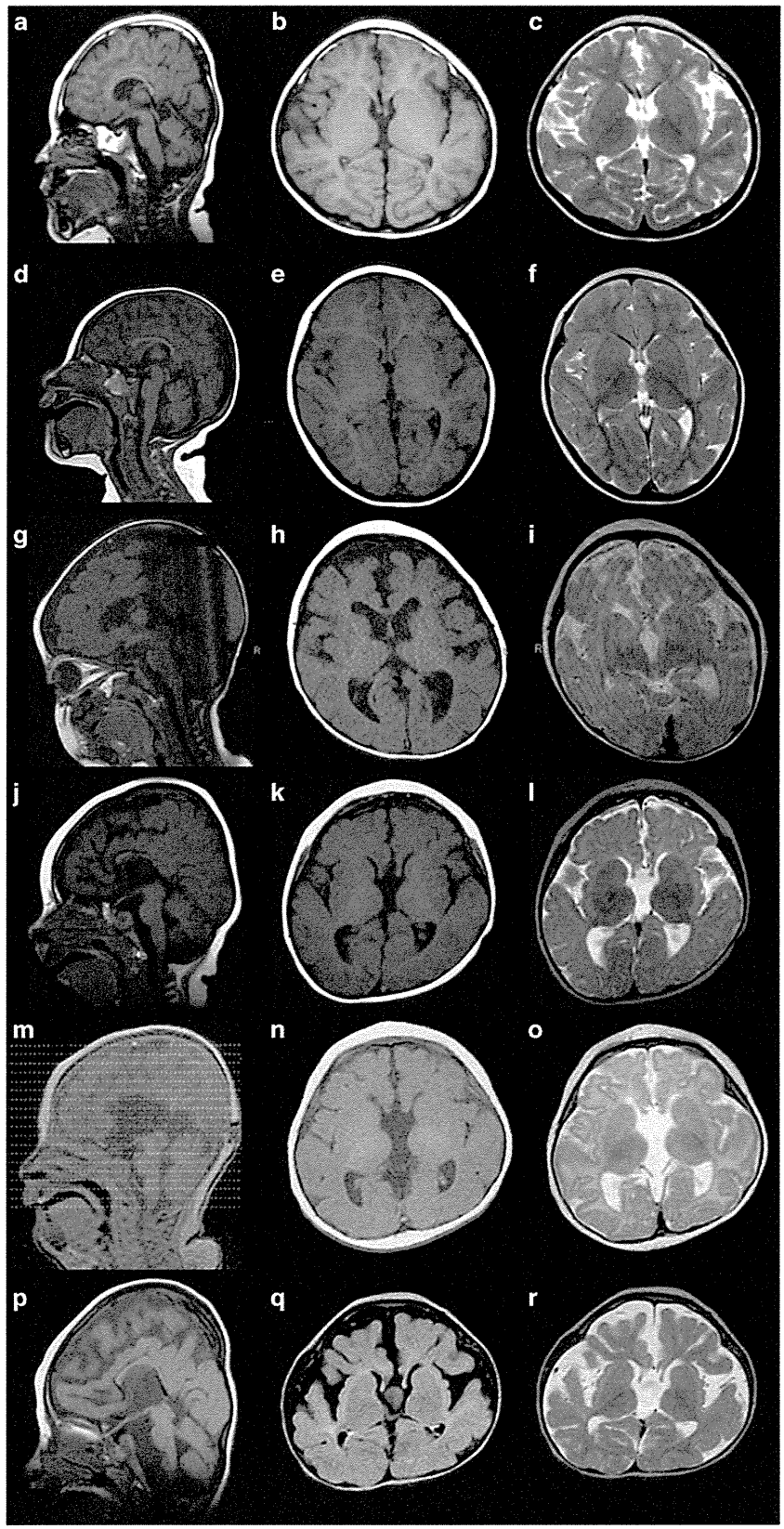

Figure 3 The brain MRI findings of patient 1 examined at 4 years (**a–c**), patient 2 examined at 3 years (**d–f**), patient 3 examined at 12 months (**g–i**), patient 4 examined at 15 months (**j–l**), patient 5 examined at 5 months (**m–o**) and patient 6 examined at 3 years (**p–r**). T1-weighted sagittal views (**a**, **d**, **g**, **j**, **m**, **p**), T1-weighted axial views (**b**, **e**, **h**, **k**, **n**, **q**) and T2-weighted axial views (**c**, **f**, **i**, **l**, **o**, **r**). ACC are noted in all patients. Patient 5 (**m**), in particular, exhibits complete agenesis of the corpus callosum. Reduced volume of the frontal lobe is seen in all patients. Prominently delayed myelination is noted in patient 3 and 4 (**i** and **l**).

triggered by hypoglycemia. Ultrasonography showed enlarged bilateral cerebral ventricles and intraventricular hemorrhage. Echocardiography showed no abnormalities. Ophthalmologic examination displayed exotropia and atrophy of the right retina and optic papilla. Auditory brain-stem response (ABR) showed normal results. Owing to her feeding difficulty, she required tube feeding. At the age of 5 months, she experienced a status convulsive epilepticus, and recurrent spike and waves were noted on EEG at that time. She was treated with several antiepileptic drugs. The brain MRI examined at 1 year of age showed ACC and reduced volume of the brain (Figures 3g–i). Low intensity of the white matter was only noted on the posterior limb of internal capsule, indicating delayed myelination (Figure 3i).

At 1 year and 6 months, the patient could not control her head by herself. She did not demonstrate eye contact, and her feeding difficulties persisted. Distinct facial features included sparse hair, microcephaly, a flat occipit, a coarse face, a high nasal bridge, low-set ears, micrognathia, inversion of eyelids, esotropia and atopic skin. Immediately after this examination, acute respiratory infectious disease caused hypoxic brain damages, which was confirmed by brain computed tomography that revealed the presence of multi-cystic lesions (data not shown). After this event, she shows spastic quadriplegia.

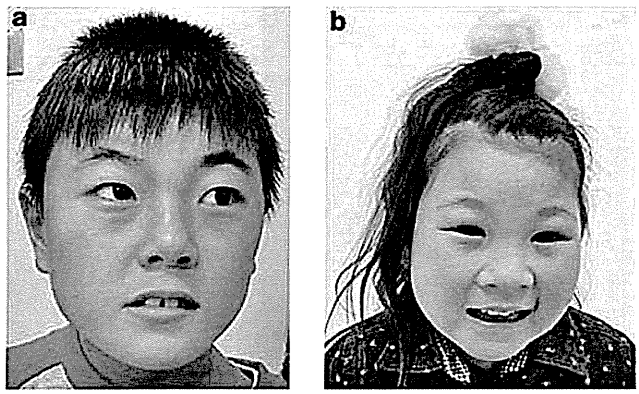

Figure 4 Facial features of patient 1 (**a**) and patient 2 (**b**). Arched eyebrows and small mouth are noted in both patients.

Patient 4

A 3-year and 3-month-old girl was born by induced delivery at 37th week as a first child of healthy, non-consanguineous parents. She showed prenatal growth retardation with her birth weight of 2386 g (<3rd centile), length of 44 cm (<3rd centile) and OFC 31 cm (<3rd centile). Atrial septal defect was revealed by ultrasonography. She displayed psychomotor developmental delay with holding up her head at 5 months, sitting by herself at 14 months and crawling at 20 months. From the age of 14 months, she was prescribed with antiepileptic drugs because of status convulsive that continued for ~1 h. The brain MRI examined at an age of 15 months revealed ACC and hypoplastic brain (Figures 3j–l). Low intensity of the white matter was only noted in the posterior limb of the internal capsule, indicating delayed myelination (Figure 3l). Conventional karyotyping on metaphase spreads prepared from peripheral lymphocytes showed a normal female karyotype.

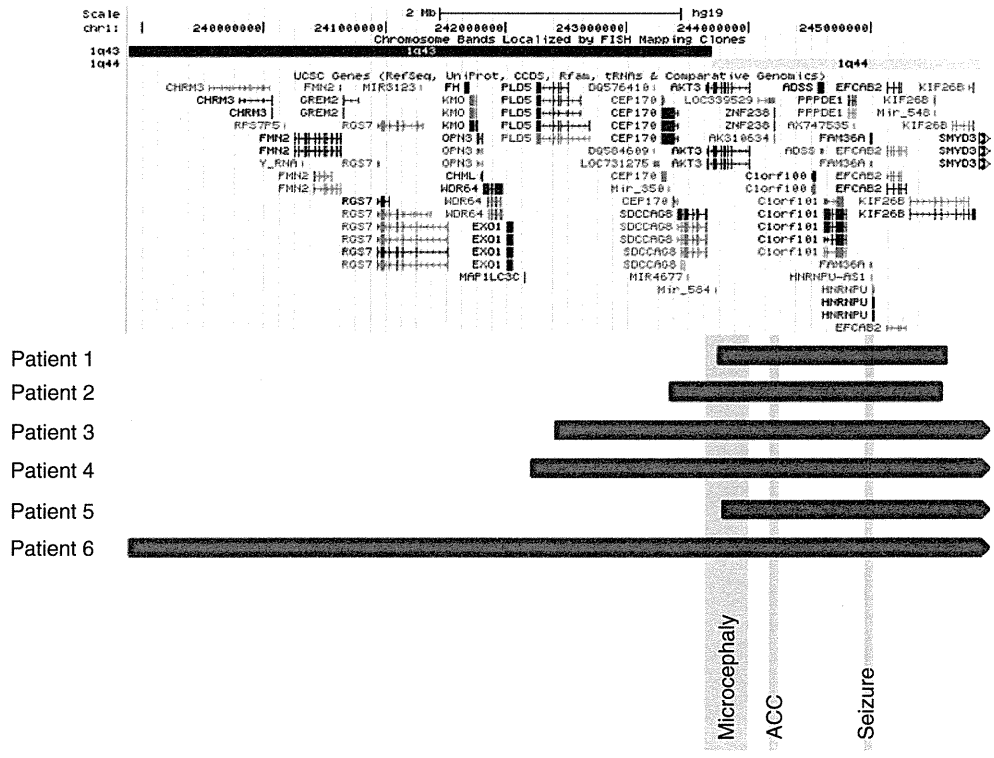

Figure 5 Deletions regions of the present patients depicted on a genome map from UCSC Genome Browser. Blue rectangles indicate the deletion region of the interstitial deletions identified on patients 1 and 2. Blue trapezoids indicate the terminal deletions identified on patients 3–6. Directions of the pointed trapezoids indicate continuous deletions to the telomeres. The region responsible for microcephaly, ACC and seizure that were proposed by Ballif *et al.*[17] are shown by gray rectangles.

Table 1 Summary of the clinical features of six patients in this study

	Patient 1	*Patient 2*	*Patient 3*	*Patient 4*	*Patient 5*	*Patient 6*	*Frequency reported by van Bon et al.*[13]
Karyotype	del (1) (q44q44)	del (1) (q43q44)	del (1) (q43)	del (1) (q43)	del (1) (q44)	del (1) (q43)	
Type of aberrations	Interstitial deletion	Interstitial deletion	Subtelomeric deletion	Unbalanced translocation	Subtelomeric deletion	Subtelomeric deletion	
Deletion region							
Start[a]	243 809 193	243 303 991	242 442 098	242 223 230	243 880 099	238 888 870	
End[a]	245 665 521	245 506 920	249 250 621	249 212 668	249 212 668	249 212 668	
Size (Mb)	1.9	2.2	6.8	7.0	5.3	10.3	
Gender	M	F	F	F	F	F	
Age	9 years	3 years and 1 month	1 year and 6 months	3 years and 3 months	6 years	10 years	
Birth weight (g)	2820	2348	2040	2386	1870	NA	
Controversial points for 1q43 deletions							
Microcephaly	+	+	+	+	+	+	9/11
Abnormalities of the corpus callosum	−	+	+	+	+	+	9/10
Seizures	+	+	+	+	+	+	9/11
Delayed myelination	−	−	+	+	NA	NA	
Severe volume loss of the brain	−	−	+	+	+	+	
General findings							
Developmental delay/mental retardation	+	+	+	+	+	+	11/11
Growth retardation	+	+	NA	+	+	+	7/11
Low birth weight	−	+	+	+	+	NA	5/11
Hypotonia	NA	+	+	NA	+	+	11/11
Feeding problem	+	−	+	−	+	NA	
Facial findings							
Round face	−	+	+	+	NA	NA	7/11
Arched eyebrows	+	+	+	+	NA	NA	
High nasal bridge	+	−	+	−	NA	NA	
Upward-slanting palpebral fissures	+	+	+	+	NA	NA	3/11
Epicanthic folds	+	+	+	+	NA	NA	4/11
Strabismus	+	−	+	−	NA	NA	2/11
Micro/retrognathia	−	−	+	+	NA	NA	0/11
Prominent jaw	+	−	−	−	NA	NA	
Low-set ears	+	+	+	+	NA	NA	
Down-turned corner of mouth	+	+	+	+	NA	NA	
Other features							
Sparse hair	−	−	+	−	NA	NA	
Flat occipit	+	−	+	−	NA	NA	
Tapering fingers	+	−	−	−	NA	NA	
Single palmer creases	+	−	−	−	NA	NA	
Complications of other organs							
Cardiac anomaly	−	−	−	ASD	−	AR	3/11
Kidney/urine pathway anomaly	−	−	−	−	Hydronephrosis	−	2/11

Abbreviations: AR, aortic regurgitation; ASD, atrial septal defect; F, female; M, male; NA, not available.
[a]Genomic positions refer to build 19.

At present, the patient exhibits severe developmental delay as she cannot stand without support and her language usage is limited to babbled words. Her mental and psychomotor developmental index of the Bayley Scales of Infant Development (II) indicate 6 and 8 months, respectively. She demonstrates growth deficiency and microcephaly with her weight of 12.8 kg (25–50th centile), height of 87.7 cm

(10th centile) and OFC of 44 cm (<3rd centile). Dysmorphic features include hypertelorism, low-set ears and micrognathia.

Patient 5

A 6-year-old girl was born at 38 weeks of gestation, with birth weight of 1870 g (<3rd centile), length of 42 cm (<3rd centile) and OFC of 28 cm (<3rd centile), indicating intrauterine growth restriction. Since early infancy, she exhibited severe hypotonia, and her psychomotor development was severely delayed. She experienced refractory seizures after 1 year of age. Although hydronephrosis was noted by abdominal ultrasonography, there was no abnormal renal function. The brain MRI examined at an age of 4 months revealed a hypoplastic brain associated with complete agenesis of the corpus callosum (Figures 3m–o). As a result of recurrent aspiration pneumonia, laryngotracheal separation surgery was performed. At present, her height is 99 cm (<3rd centile), weight is 15.3 kg (<3rd centile) and OFC of 42 cm (<3rd centile), indicating severe growth deficiency and microcephaly. She can stand by support, but no meaningful words.

Patient 6

A 10-year-old girl was born at 40 weeks and 3 days of gestation. At the age of 3 years, she was referred to our institution because of intractable epilepsy. At that time, neurological examination revealed generalized hypotonia. EEG showed frequent spikes on the left hemisphere. The brain MRI indicated a hypoplastic brain associated with ACC and delayed myelination (Figures 3p–r). Echocardiography revealed mild aortic regurgitation. At present, her height is 115 cm (<3rd centile), weight is 16.3 kg (<3rd centile) and OFC of 48 cm (<3rd centile), indicating growth delay and microcephaly. She shows severe psychomotor developmental delay with sitting by support and no meaningful word.

DISCUSSION

The characteristics of 1q44 deletions have been recognized as growth deficiency, psychomotor developmental delay, epilepsy, microcephaly, brain malformations including ACC, and distinct facial features.[4,6,7,9,11,18] After chromosomal microarray testing has been available for the identification of submicroscopic chromosomal aberrations, many patients with submicroscopic deletions of 1q44 have been identified.[8,10,12,14,15] Now, precise genotype–phenotype correlation has been evaluated through the accumulation of patients with variable deletion sizes, and a minimal essential region has been proposed for expressing the main characteristics of 1q44 deletion syndrome.[7,8,14–16] Ballif *et al.*[17] evaluated 22 patients with small interstitial deletions of 1q44 and demonstrated critical regions for microcephaly, ACC and seizures. Consequently, *AKT3* was reported to be the gene responsible for microcephaly; zinc finger protein 238 gene (*ZNF238*) for ACC; and heterogeneous nuclear ribonucleoprotein U gene (*HNRNPU*) for seizures[17] (Figure 5).

In this study, we identified six patients with the deletions including 1q44. Clinical and genetic findings were summarized in Table 1 and Figure 5, respectively. The presenting patient 1 and 2 showed typical interstitial deletions of 1q44, in which *AKT3* and *ZNF238* are included, and manifested the typical features of mental retardation, microcephaly, ACC and seizures. This evidence supports the findings reported by Ballif *et al.* that the essential features of 1q44 deletion syndrome are derived from deletions of the minimal region including *AKT3* and *ZNF238*.[17] In comparison with these two patients, the other four patients displayed terminal deletion of 1q44 that include the minimal region including *AKT3* and *ZNF238*. Although the chromosomal breakpoint of patient 5 was just on *AKT3*, phenotypic feature of this patient are extremely severe as compared with those of patient 1 and 2 who had interstitial deletion of 1q44. Although Roos *et al.*[18] reported that 1.6 Mb terminal region does not have clinical relevance, because it appears to primarily contain many of the olfactory receptors genes, many genes of unknown functions are included in this 2.6 Mb region (chr1:245 000 000–247 600 000). Thus, this additionally deleted region in patient 5 may also have been responsible for his severe neurological manifestations.

Patient 4 had an additional chromosomal aberration, with a partial trisomy of 5p derived from an unbalanced translocation. However, the phenotypic severity of patient 4 was not significantly different from that of the other patients with 1q43 deletions. Thus, the partial trisomy of 5p identified in patient 4 did not demonstrate an important contribution to the patient's manifestations. Patient 3 showed extremely severe developmental delay, which may have been modified by the hypoglycemia and subsequent intraventricular hemorrhage suffered during the early infantile period.

The deletion regions of the remaining three patients (patient 3, 4 and 6) expanded toward the centromere beyond the critical region for 1q44 deletion syndrome, and several more genes are included in the deletion region in these three patients. Severe volume loss of the brain was revealed in the brain MRI of these three patients, similar to patient 5, and delayed myelination was also seen on the brain MRI of patient 3 and 4 (Figures 3i, l). Although patient 5 exhibited high T2 signal intensities in the white matter, this image was obtained when he was 4 months of age, and we cannot ascertain if this finding indicated delayed myelination. Similarly, because the brain MRI of patient 1, 2 and 6 were obtained after 3 years of age, we cannot determine whether these three patients experienced delayed myelinations in their early infancy. However, delayed myelination, as a finding associated with 1q44 deletion, has not yet been reported in the literature.[17] It may therefore be that the characteristic findings of the patients with expanded deletion beyond the 1q43 region may have clinical implications for delayed myelination. Although many UCSC genes are present in these additional regions, some of these genes may have clinical relevance for delayed myelination observed in patient 3 and 4. The centrosomal protein 170 kDa gene (*CEP170*) is a potential candidate because of its high expression level in the fetal brain.

In this genotype–phenotype correlation study for patients with 1q44 deletions, we revealed that telemetric region beyond the physical position of chr1:245 000 000 may be responsible for severe volume loss of the brain, and the proximal region beyond *AKT3* may be responsible for delayed myelination. The neighboring genes surrounding 1q43q44 may have some modifier effects to the severe brain impairments associated with delayed myelination. To identify them, much more information regarding genotype–phenotype correlations will need to be accumulated for patients with terminal deletion of 1q.

CONFLICT OF INTEREST

The authors declare no conflict of interest.

ACKNOWLEDGEMENTS

We thank the patients and their parents for their gracious participation and support. This work was supported by Grant-in-Aid for Research Activity Start-up for KS and Grant-in-Aid for Scientific Research (C) for TY from the Japan Ministry of Education, Science, Sports and Culture.

1 Knight, S. J., Regan, R., Nicod, A., Horsley, S. W., Kearney, L., Homfray, T. *et al.* Subtle chromosomal rearrangements in children with unexplained mental retardation. *Lancet* **354,** 1676–1681 (1999).
2 Shimojima, K., Sugiura, C., Takahashi, H., Ikegami, M., Takahashi, Y., Ohno, K. *et al.* Genomic copy number variations at 17p13.3 and epileptogenesis. *Epilepsy Res.* **89,** 303–309 (2010).
3 Cardoso, C., Leventer, R. J., Ward, H. L., Toyo-Oka, K., Chung, J., Gross, A. *et al.* Refinement of a 400-kb critical region allows genotypic differentiation between isolated lissencephaly, Miller-Dieker syndrome, and other phenotypes secondary to deletions of 17p13.3. *Am. J. Hum. Genet.* **72,** 918–930 (2003).
4 Gentile, M., Di Carlo, A., Volpe, P., Pansini, A., Nanna, P., Valenzano, M. C. *et al.* FISH and cytogenetic characterization of a terminal chromosome 1q deletion: clinical case report and phenotypic implications. *Am. J. Med. Genet. A* **117A,** 251–254 (2003).
5 Puthuran, M. J., Rowland-Hill, C. A., Simpson, J., Pairaudeau, P. W., Mabbott, J. L., Morris, S. M. *et al.* Chromosome 1q42 deletion and agenesis of the corpus callosum. *Am. J. Med. Genet. A* **138,** 68–69 (2005).
6 van Bever, Y., Rooms, L., Laridon, A., Reyniers, E., van Luijk, R., Scheers, S. *et al.* Clinical report of a pure subtelomeric 1qter deletion in a boy with mental retardation and multiple anomalies adds further evidence for a specific phenotype. *Am. J. Med. Genet. A* **135,** 91–95 (2005).
7 Boland, E., Clayton-Smith, J., Woo, V. G., McKee, S., Manson, F. D., Medne, L. *et al.* Mapping of deletion and translocation breakpoints in 1q44 implicates the serine/threonine kinase AKT3 in postnatal microcephaly and agenesis of the corpus callosum. *Am. J. Hum. Genet.* **81,** 292–303 (2007).
8 Hill, A. D., Chang, B. S., Hill, R. S., Garraway, L. A., Bodell, A., Sellers, W. R. *et al.* A 2-Mb critical region implicated in the microcephaly associated with terminal 1q deletion syndrome. *Am. J. Med. Genet. A* **143A,** 1692–1698 (2007).
9 Merritt, II J. L., Zou, Y., Jalal, S. M. & Michels, V. V. Delineation of the cryptic 1qter deletion phenotype. *Am. J. Med. Genet. A* **143,** 599–603 (2007).
10 Andrieux, J., Cuvellier, J. C., Duban-Bedu, B., Joriot-Chekaf, S., Dieux-Coeslier, A., Manouvrier-Hanu, S. *et al.* A 6.9 Mb 1qter deletion/4.4 Mb 18pter duplication in a boy with extreme microcephaly with simplified gyral pattern, vermis hypoplasia and corpus callosum agenesis. *Eur. J. Med. Genet.* **51,** 87–91 (2008).
11 Hiraki, Y., Okamoto, N., Ida, T., Nakata, Y., Kamada, M., Kanemura, Y. *et al.* Two new cases of pure 1q terminal deletion presenting with brain malformations. *Am. J. Med. Genet. A* **146A,** 1241–1247 (2008).
12 Poot, M., Kroes, H. Y. & Hochstenbach, R. AKT3 as a candidate gene for corpus callosum anomalies in patients with 1q44 deletions. *Eur. J. Med. Genet.* **51,** 689–690 (2008).
13 van Bon, B. W., Koolen, D. A., Borgatti, R., Magee, A., Garcia-Minaur, S., Rooms, L. *et al.* Clinical and molecular characteristics of 1qter microdeletion syndrome: delineating a critical region for corpus callosum agenesis/hypogenesis. *J. Med. Genet.* **45,** 346–354 (2008).
14 Orellana, C., Rosello, M., Monfort, S., Oltra, S., Quiroga, R., Ferrer, I. *et al.* Corpus callosum abnormalities and the controversy about the candidate genes located in 1q44. *Cytogenet. Genome Res.* **127,** 5–8 (2009).
15 Caliebe, A., Kroes, H. Y., van der Smagt, J. J., Martin-Subero, J. I., Tonnies, H., van't Slot, R. *et al.* Four patients with speech delay, seizures and variable corpus callosum thickness sharing a 0.440 Mb deletion in region 1q44 containing the HNRPU gene. *Eur. J. Med. Genet* **53,** 179–185 (2010).
16 Nagamani, S. C., Erez, A., Bay, C., Pettigrew, A., Lalani, S. R., Herman, K. *et al.* Delineation of a deletion region critical for corpus callosal abnormalities in chromosome 1q43-q44. *Eur. J. Hum. Genet.* **20,** 176–179 (2012).
17 Ballif, B. C., Rosenfeld, J. A., Traylor, R., Theisen, A., Bader, P. I., Ladda, R. L. *et al.* High-resolution array CGH defines critical regions and candidate genes for microcephaly, abnormalities of the corpus callosum, and seizure phenotypes in patients with microdeletions of 1q43q44. *Hum. Genet.* **131,** 145–156 (2012).
18 Roos, A., Eggermann, T., Zerres, K. & Schuler, H. M. Polymorphic subtelomeric deletion 1q demonstrates the need to reevaluate subtelomere screening methods: determination of the boundary between pathogenic deletion and benign variant for subtelomere 1q. *Am. J. Med. Genet. A* **146A,** 795–798 (2008).

Supplementary Information accompanies the paper on Journal of Human Genetics website (http://www.nature.com/jhg)

RESEARCH ARTICLE

AMERICAN JOURNAL OF medical genetics PART A

Clinical and Radiological Features of Japanese Patients With a Severe Phenotype due to *CASK* Mutations

Jun-ichi Takanashi,[1,2]* Nobuhiko Okamoto,[3] Yuto Yamamoto,[3] Shin Hayashi,[4] Hiroshi Arai,[5] Yukitoshi Takahashi,[6] Koichi Maruyama,[7] Seiji Mizuno,[7] Shuichi Shimakawa,[8] Hiroaki Ono,[9] Reiki Oyanagi,[10] Satomi Kubo,[11] A. James Barkovich,[12] and Johji Inazawa[4]

[1]Department of Pediatrics, Kameda Medical Center, Kamogawa, Japan

[2]Department of Radiology, Toho University Sakura Medical Center, Sakura, Japan

[3]Department of Medical Genetics, Osaka Medical Center and Research Institute for Maternal and Child Health, Osaka, Japan

[4]Department of Molecular Cytogenetics, Medical Research Institute and School of Biomedical Science, Tokyo Medical and Dental University, Tokyo, Japan

[5]Department of Pediatric Neurology, Morinomiya Hospital, Osaka, Japan

[6]National Epilepsy Center, Shizuoka Institute of Epilepsy and Neurological Disorders, Shizuoka, Japan

[7]Department of Pediatric Neurology, Aichi Prefectural Colony Central Hospital, Kasugai, Japan

[8]Department of Pediatrics, Osaka Medical College, Takatsuki, Japan

[9]Department of Pediatrics, Hiroshima Prefectural Hospital, Hiroshima, Japan

[10]Department of Pediatrics, Hokkaido Medical Center for Child Health and Rehabilitation, Sapporo, Japan

[11]Department of Pediatrics, Nara Prefectural Nara Hospital, Nara, Japan

[12]Department of Radiology and Biomedical Imaging, University of California San Francisco, California

Manuscript Received: 31 March 2012; Manuscript Accepted: 5 August 2012

Heterozygous loss of function mutations of *CASK* at Xp11.4 in females cause severe intellectual disability (ID) and microcephaly with pontine and cerebellar hypoplasia (MICPCH). However, the longitudinal clinical and radiological course of affected patients, including patterns of postnatal growth, has not been described. Neurodevelopmental and imaging information was retrospectively accrued for 16 Japanese (15 female and 1 male) patients with ID and MICPCH associated with *CASK* mutations. All records were analyzed; patient age ranged from 2 to 16 years at the time of the most recent examinations. The growth pattern, neurological development, neurological signs/symptoms, and facial features were similar in the 15 female patients. Their head circumference at birth was within the normal range in about half, and their height and weight were frequently normal. This was followed by early development of severe microcephaly and postnatal growth retardation. The patients acquired head control almost normally between 3 and 6 months, followed by motor delay. More than half of the female patients had epilepsy. Their MRIs showed microcephaly, brainstem, and cerebellar hypoplasia in early infancy, and a normal or large appearing corpus callosum. The male patient showed a more severe clinical phenotype. These uniform clinical and radiological features should facilitate an early diagnosis and be useful for medical care of females with ID and MICPCH associated with *CASK* mutations.

How to Cite this Article:
Takanashi J-i, Okamoto N, Yamamoto Y, Hayashi S, Arai H, Takahashi Y, Maruyaa K, Mizuno S, Shimakawa S, Ono H, Oyanagi R, Kubo S, Barkovich AJ, Inazawa J. 2012. Clinical and radiological features of Japanese patients with a severe phenotype due to *CASK* mutations.
Am J Med Genet Part A 158A:3112–3118.

Grant sponsor: Research Grant for Nervous and Mental Disorders, Ministry of Health, Labor and Welfare of Japan; Grant number: 24-7; Grant sponsor: Grant-in-Aid for Scientific Research (C), JSPS; Grant number: 24591790; Grant sponsor: Health and Labor Sciences Research Grants, Ministry of Health, Labor and Welfare of Japan; Grant sponsor: New Energy and Industrial Technology Development Organization (NEDO).
The authors declared that they have no conflicts of interest.
*Correspondence to:
Jun-ichi Takanashi, Department of Pediatrics, Kameda Medical Center, 929 Higashi-cho, Kamogawa-shi, Chiba 296-8602, Japan.
E-mail: jtaka44@hotmail.co.jp
Article first published online in Wiley Online Library (wileyonlinelibrary.com): 19 November 2012
DOI 10.1002/ajmg.a.35640

Key words: *CASK*; Intellectual disability; microcephaly; pontine hypoplasia; cerebellar hypoplasia; epilepsy; MRI

INTRODUCTION

The CASK protein belongs to the membrane-associated guanylate kinase protein family, functioning as a multi-domain scaffolding protein, and plays important roles in neural development and synaptic function [Hsueh, 2006, 2009; Hayashi et al., 2008; Najm et al., 2008]. It has been reported that *CASK* aberrations can cause three clinical phenotypes, severe intellectual disability (ID) and microcephaly with pontine and cerebellar hypoplasia (MICPCH, OMIM: #300749) in females [Takanashi et al., 2010; Moog et al., 2011; Hayashi et al., 2012], mild to severe ID with or without nystagmus, microcephaly, and/or dysmorphic features in males [Hackett et al., 2010], and FG syndrome in males [Piluso et al., 2009] depending on the type of aberration of the gene [Moog et al., 2011; Hayashi et al., 2012]. Hypomorphic missense mutations of *CASK* in males probably cause FG syndrome or mild to severe ID with or without nystagmus, microcephaly, and/or dysmorphic features, whereas *CASK* null mutations (haploinsufficiency of *CASK*) in females cause ID and MICPCH [Moog et al., 2011; Hayashi et al., 2012]. This theory explains the similarity of the clinical and radiological phenotypes of ID and MICPCH regardless of the type of *CASK* mutation [Takanashi et al., 2010; Moog et al., 2011; Hayashi et al., 2012]; however, no long-term clinical and radiological information has been published on this group of patients. We present clinical and radiological evaluations of 16 Japanese patients with ID and MICPCH associated with *CASK* mutations.

MATERIALS AND METHODS

Sixteen Japanese patients (15 female and 1 male, 2–16 years old) clinically diagnosed with ID and MICPCH and confirmed to have *CASK* mutations were enrolled in this study. Written informed consent for genetic and clinical analysis was obtained from the parents after institutional review board approval was obtained from Tokyo Medical and Dental University and Kameda Medical Center. Genetic analysis and brief clinical features of 10 of the 16 patients [Hayashi et al., 2012], and magnetic resonance imaging (MRI) features of 5 of the 16 patients [Takanashi et al., 2010] were previously reported, respectively. The 15 female patients most likely have *CASK* loss-of-function mutations [Hayashi et al., 2012], which are expected to cause a characteristic pattern of ID and MICPCH in females [Moog et al., 2011; Hayashi et al., 2012]. In silico prediction programs and splice site prediction software showed that the de novo mutation in a male (Patient 16), situated in an important interaction domain of CASK, was considered to damaging to protein function, and this position was not associated with a splice site. We reviewed all available data, including MRI scans, raw data from the MRIs for use in quantification, and information concerning growth, development, and neurologic status. Height, weight, and head circumference were measured in all patients at birth, and subsequently recorded two to five times for female patients, and six times for the male. The MRI data with 1.5 T magnet were used to quantify the area of the cerebrum, cerebellar hemispheres, pons, and corpus callosum in each patient using the same methods previously reported [Takanashi et al., 2010]; patients ranged in age from 4 to 156 months at the time of their MRI. One (Patient 11) was scanned three times at ages 9, 24, and 50 months. The results of these measurements were compared with those of 62 female patients (0.5–180 months old) evaluated at the Kameda Medical Center using 1.5 T Siemens apparatus for mild neurological symptoms, such as headache, hypotonia, seizures, febrile delirium, or mild asphyxia, who had no parenchymal lesion on MRI, and showed normal subsequent neurodevelopmental exams; as well as those of five patients with pontine hypoplasia due to causes other than *CASK* mutations, including PEHO [Tanaka et al., 1997], 5p-syndrome [Ninchoji and Takanashi, 2010], and trisomy 18 (disease controls).

RESULTS

Clinical Records

The epilepsy and genetic data of the 16 patients with ID and MICPCH associated with *CASK* mutations are summarized in Table I. Postnatal growth curves are shown in Figure 1 (head circumference in Fig. 1a; height and weight in Fig. 1b,c). Fifteen patients were born at term (>37 weeks gestation); mean OFC was 30.4 ± 1.7 (mean ± SD) cm, height was 47.0 ± 2.6 cm, and weight was 2640 ± 420 g. Patient 5 was born at 33 weeks' gestation with an OFC of 28.0 cm, height of 41.4 cm, weight of 1596 g. Microcephaly, defined as less than the third centile (30.2 cm), was present at birth in 7/15 (47%) patients born at term. Microcephaly was recognized in all patients examined after age 4 months, with OFC measuring below −4 SD, including a male patient (Fig. 1, stars) and a female born at 33 weeks. Height at birth was low normal (within 2 SD) in 13/15 patients born at term, declining to around the −2 SD level after 4 years, and below the −3 SD level after 8 years. Birth weight was normal or low normal in 14/15 patients born at term, decreasing to the −1 SD to −2 SD level after 4 months, and around the −2 SD after 2 years. Height and weight of a male patient (Fig. 1, stars) and a female born at 33 weeks overlapped those of females born at term.

Hypotonia was observed in 11/16, muscle weakness in 10/16, spasticity or increased deep tendon reflexes in 12/16, involuntary movements in 3/16, sensory deafness in 2/16, and ophthalmologic anomalies in 3/16 (abnormal visual evoked potentials, strabismus, and nystagmus), respectively. Four patients presented with hypohidrosis, and two of these also showed hyposensitivity to pain. A typical facial appearance (Fig. 2) was noted (including the male patient, Fig. 2b), with an oval face in all patients, large eyes, or irises in 13/16, large ears in 11/16, a broad nasal bridge in 14/16, a broad nasal tip in 9/16, a small nose in 6/16, epicanthal folds in 5/16, a small jaw in 11/16, a long philtrum in 7/16, and a high-arched palate in 7/16.

The motor milestones are shown in Figure 3. The male (Patient 16) showed no psychomotor development at 5 years old, that is, he could not control his head, smile, or babble. The 15 female patients exhibited early psychomotor development; all

TABLE I. Features of Epilepsy in Patients With ID and MICPCH Associated With *CASK* Mutations.

Pt	Age (Mo)	M/F	Epilepsy/seizure type	Onset (Mo)	EEG	Therapy	Response	*CASK* mutation
1	190	F	GE/atonic	65	bil. F. and diffuse slow SWC	VPA, CZP, ESM	PR	Pt. No. in Hayashi et al. [2012]
2	42	F						c.2302 + delT
3	33	F	ES, CPS	17	bil. F. spikes			c.173_173 + 1gelGG
4	24	F				VPA, ACTH, TPM, LTG	Intractable	c.316C > G p.Arg106Stop
5	95	F	LGS/atonic, myoclonic, spasms	43	diffuse slow SWC			c.1910G > A p.Gly637Asp
6	147	F	CPS	17	left O. SWC	VPA, CLB, TPM, LTG	CR	del(X)(p11.3p11.4)
7	63	F			Normal	VPA, GBP	PR	9
8	111	F	FLE	60	bil. F. spikes			3
9	61	F				VPA, CBZ	CR	10
10	36	F	ES	34	Normal			1
11	49	F				VPA	CR	4
12	124	F	EMA	108	bil. F. SWC, bil. P.O. spikes			8
13	194	F	GE/tonic	130	left C.P., right C.P. spikes	VPA, CZP, ESM	Intractable	5
14	184	F			Normal	VPA	CR	7
15	27	F						6
16	63	M	WS, GE/tonic, myoclonic	4	4 Mo hyps, 5 years left F.C. spikes			2
						ACTH, VPA, PHT	Intractable	c.1061T > C p.Leu348Pro

Abbreviations: Pt, patient; M, male; F, female; Mo, month; GE, generalize epilepsy; ES, epileptic spasms; CPS, complex partial seizure; LGS, Lennox–Gastaut syndrome; FLE, frontal lobe epilepsy; EMA, epilepsy with myoclonic absences; WS, West syndrome; bil, bilateral; F, frontal; SWC, spike and wave complex; O, occipital; P, parietal; C, central; hyps, hypsarrhythmia; VPA valproate; CLB clobazam; TPM, topiramate; LTG, lamotrigine; GBP, gabapentin; CBZ, carbamazepine; ESM, ethosuximide; ACTH, adrenocorticotropic hormone; PHT, phenytoin; PR, partial remission, CR, complete remission.

could control their head at ages 3–6 (4.6 ± 1.2) months. Sitting independently was possible in 13/15 patients between 7 and 25 (14.2 ± 5.7) months, and walking independently in five between 29 and 72 months. All 15 female patients could smile, only four could babble, and one could utter a word.

The male patient presented with West syndrome (epileptic spasms and hypsarrhythmia) at 4 months, followed by generalized epilepsy, which was intractable to antiepileptic drugs. Eight of the 15 female patients (53%) had epilepsy, with onset between 17 and 130 (mean, 60) months, including two with epileptic spasms (no hypsarrhythmia), one with Lennox–Gastaut syndrome. EEG showed variable abnormalities, the most common finding being bilateral frontal spikes or spike and wave complexes in four patients. The response to antiepileptic drugs was also variable.

MRI Findings

The representative MRI (Fig. 4) and MRI measurements (areas of cerebrum, cerebellar hemispheres, pons, and corpus callosum), and the cerebrum/corpus callosum ratio of the controls and patients are shown in Figure 5. The areas of all measured regions increased with increasing age in the controls, whereas the cerebrum/corpus callosum ratio decreased with age, reaching the adult value at around age 5 years. In the CASK patients, the area of the cerebrum,

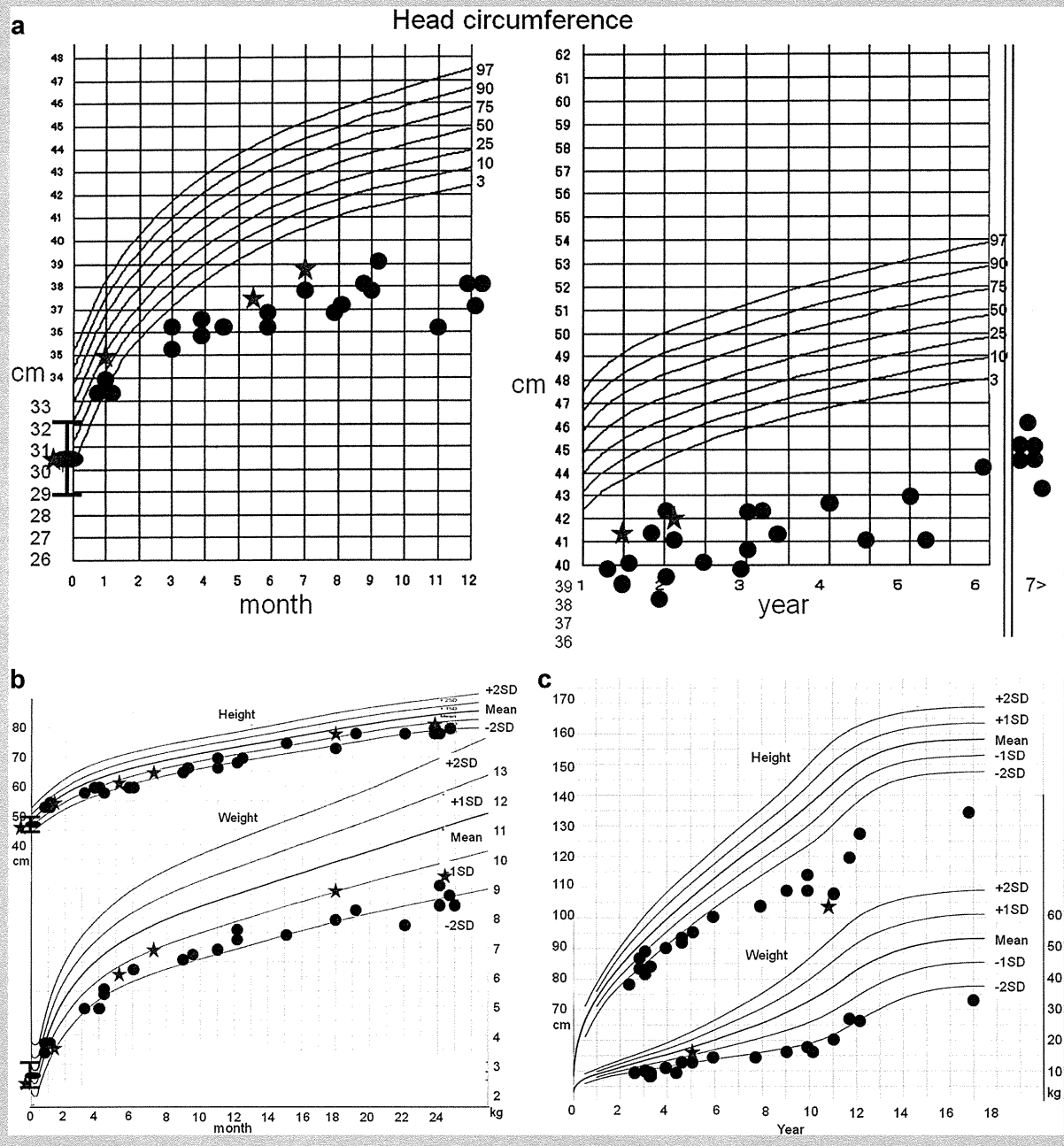

FIG. 1. Growth curves for head circumference (a), height, and weight (b,c). Black circles represent female patients, and stars a male patient. Large circle with bars represent mean ± standard deviation at birth.

cerebellar hemispheres, and pons (Fig. 5a–c) were much reduced in size when compared to controls, even in early infancy (after 4 months), and showed little size increase with age. The midline corpus callosum area was normal or in the low-normal range in all patients (Fig. 5d), appearing abnormally thick compared to the small cerebrum. The cerebellum/corpus callosum ratio was low normal or low in all patients with ID and MICPCH associated with *CASK* mutations (Fig. 5e). No obvious malformations were seen in the cerebral hemispheres in the 16 patients. In all five patients with non-*CASK*-related pontine hypoplasia, the corpus callosum was reduced in size and the cerebrum/corpus callosum ratio was high.